Turkish Journal of Chemistry
http://journals.tubitak.gov.tr/chem/
Research Article

Turk J Chem
(2018) 42: 247 – 256

doi:10.3906/kim-1706-12

Effect of pH and β-cyclodextrin on the photophysical properties of lamotrigine

Raed GHANEM[1,*], **Fakhri YOUSEF**[2], **Omar ABU AWWAD**[1]
[1]Department of Chemistry, Al Al-Bayt University, Mafraq, Jordan
[2]Department of Chemistry, Al-Hussein Bin Talal University, Ma'an, Jordan

Received: 06.06.2017 • **Accepted/Published Online:** 05.09.2017 • **Final Version:** 27.04..2018

Abstract: Photophysical properties of lamotrigine (LMT) were investigated at different pH values. Lamotrigine exhibited a broad absorption band at 308 nm that was shifted to 268 nm at pH 2.0 due to protonation (HLMT+). Emission spectra of LMT at different pH values showed a single band at 483 nm except for at pH 2.0, where a second band at 502 nm was observed due to the deprotonation from the singlet excited state. LMT pH profile was used to calculate pKa of LMT in excited and ground states (pKa* = 4.50 and pKa = 5.90). Absorption spectra of LMT at different pH values for LMT in the presence of β-CD showed an isosbestic point at 290 nm. A significant enhancement in the emission intensity of LMT upon increasing β-CD (0–7 mmol L^{-1}) was reported. Benesi–Hildebrand analysis showed that LMT/β-CD and HLMT+/β-CD complexes have 1:1 stoichiometry, with K11 values ranging from 122 at pH 2.0 to 50 at pH 8.0. Thermodynamic parameters showed that complexation process is enthalpy driven (ΔH$^\circ$ = −23.1 kJ.mol^{-1} at pH 2.0 and –24.1 kJ.mol^{-1} at pH 8.0). Molecular mechanical calculations by MM+ force field indicated that LMT is preferentially included within the β-CD cavity through its diamino-1,2,4-triazine moiety.

Key words: Lamotrigine, photophysical properties, β-cyclodextrin, effect of pH, Benesi–Hildebrand analysis

1. Introduction

Lamotrigine (LMT) (Figure 1) is 3,5-diamino-6-(2,3-dichlorophenyl)-1,2,4-triazine, used in the treatment of complex partial and generalized tonic–clonic seizures. LMT acts by blocking voltage-gated sodium channels to stabilize the presynaptic neuronal membrane and inhibit the presynaptic release of glutamate.[1−3]

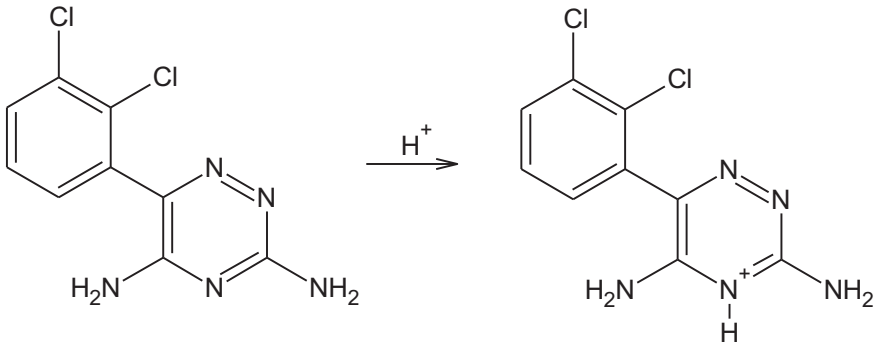

Figure 1. Structural formula and protonation site of LMT.

*Correspondence: raedag@aabu.edu.jo

Cyclodextrins (CDs) are cyclic oligosaccharides containing six (α-CD), seven (β-CD), and eight (γ-CD) (α-1,4)-linked α-D-glucopyranose units. The truncated cone shape CDs have the primary hydroxyl groups at the narrow rim and secondary hydroxyl groups at the wide rim, leaving a hydrophobic interior cavity that can include suitably sized organic molecules.[4] The chemical and spectroscopic properties of guest molecules are modified as a result of the inclusion within CD cavities due to variation in the microenvironment experienced by the included guest. Upon inclusion within the CD cavity, a noticeable change is usually observed in the spectrofluorimetric properties of the included molecules including fluorimetric intensity enhancement[5–7] and increase in the fluorescence lifetime.[8,9]

Complexation of LMT with CDs was investigated only by some workers, as part of formulation studies, where dissolution rates were improved through complexation and apparent complex formation constants were evaluated through phase-solubility diagrams.[10,11] To the best of our knowledge, no adequate fluorimetric evaluation for LMT was found in the literature except for the LMT photodegradation study performed in simulated sunlight by Young et al.[12] A spectrofluorimetric technique was utilized only as a sensitive analysis technique for the determination of LMT in human plasma.[13] Moreover, no adequate evaluation of the effect of β-cyclodextrin (used as an excipient in drug formulations) on the fluorimetric properties of LMT was reported. If β-cyclodextrin is used in any LMT formulation, the complex will exist at different pH values in the human body (pH 1.5 in the stomach up to pH 8.5 in the duodenum end of the body); therefore, the goal of our study was to evaluate the effect of β-cyclodextrin on the fluorimetric properties of LMT in a pH range similar to that found in the human body (pH 2.0–8.0)

The present work investigated the effect of pH and β-CD on the photophysical properties of LMT using UV-absorption and steady-state fluorescence emission measurements. A detailed investigation of LMT/β-CD complex formation was also conducted.

2. Results and discussion

2.1. Spectroscopic and photophysical properties of LMT

The absorption and emission spectroscopic behavior of LMT in buffered aqueous solutions at pH 2.0 (100% protonated LMT; $HLMT^+$); pH 4.0, 5.0, and 6.0 (partially protonated LMT); and pH 8.0 (neutral LMT) were investigated at 298.0 K. Neutral LMT (at pH 8.0) was found to have a maximum absorption peak at about 308 nm, which shifted to about 268 nm upon protonation (at pH 2.0) (Figure 2), in good agreement with what was reported elsewhere.[12,14] This large UV-absorption shift of about 40 nm can be attributed to the protonation of the most basic 4-N- position of the substituted 1,2,4-triazine ring moiety as shown in Figures 1 and 2. For partially protonated LMT, the maximum absorption peak occurs at wavelengths between 268 nm and 308 nm depending on the degree of protonation, i.e. pH value.

Fluorescence emission spectra have a maximum emission wavelength at 483 nm for neutral or partially protonated LMT. The fluorescence spectrum of $HLMT^+$ (at pH 2.0) consists of two emission bands; the band at the shorter wavelength of 380 nm corresponds to the acidic protonated form $HLMT^+$, while that at 502 nm can be ascribed to the neutral form. As can be seen in the Scheme, this fluorescence behavior in aqueous solutions results from the deprotonation that occurs in the excited singlet state of $HLMT^+$ to give neutral LMT and hydrated protons.[15–17] At pH 2.0, the maximum emission shifted to 502 nm with a slight increase in fluorescence intensity (Figure 3), which indicates that the quenching process of the singlet excited state, after deprotonation, is less efficient.

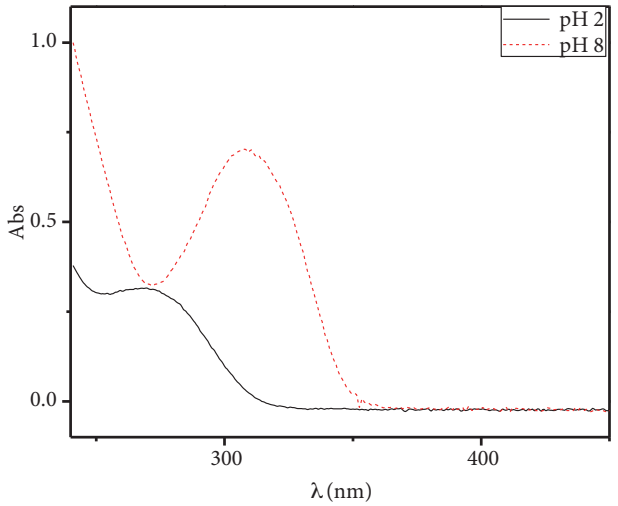

Figure 2. Absorption spectra of 5.0 × 10^{-5} mol L^{-1} LMT in 0.10 mol L^{-1} phosphate buffer at pH 2.0 and pH 8.0.

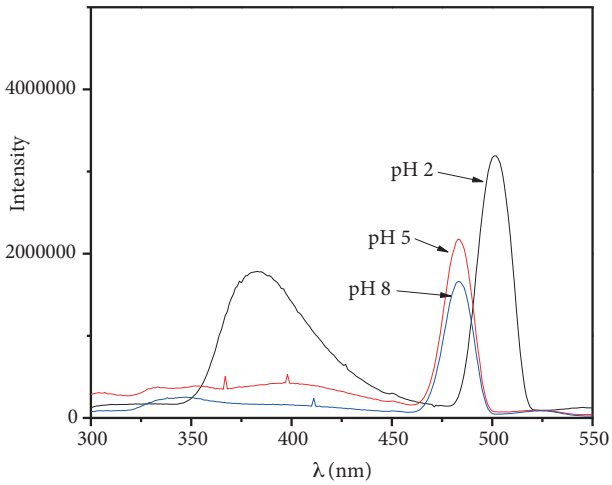

Figure 3. Fluorescence emission spectra of 5.0 × 10^{-5} mol L^{-1} LMT in 0.10 mol L^{-1} phosphate buffer at pH 2.0, pH 5.0, and pH 8.0. $\lambda_{excitation}$ = 280 nm.

$$HLMT^{+} \xrightarrow{h\nu} HLMT^{+*} \xrightarrow{H_2O} LMT^{*} + H_3O^{+} \rightarrow LMT + h\nu\,(502\,nm)$$

Scheme. Deprotonation scheme for $HLMT^{+}$ excited singlet state.

Figure 4 shows the plot of β_{max} of LMT at different pH values, where the pH at the inflection point of the sigmoidal curve equals the pK_a value. The ground state acidity constant of $HLMT^{+}$ LMT equilibrium was determined to be 5.90 ± 0.04, which is in good agreement with previously reported values.[14–16] The pK_a^* value for the monocation-neutral equilibrium in the singlet excited state S_1 was determined using fluorescence emission spectra at different pH values and found to be 4.50 ± 0.07 (Figure 5). This increase in acidity (pK_a^* < pK_a) results from an intramolecular proton transfer in the excited state.[18,19]

2.2. Effect of β-CD on the spectral properties of LMT

Absorption and fluorescence emission spectra were obtained for LMT in buffered aqueous solutions at different β-CD concentrations at pH values 2.0, 4.0, 5.0, 6.0, and 8.0. Upon addition of β-CD to aqueous solutions of LMT, a slight blue shift of the UV absorption bands was observed for neutral LMT (306 nm at pH 8.0) and for protonated LMT (265 nm at pH 2.0). An absorbance enhancement was noted for $HLMT^{+}$ solutions upon complexation with β-CD at pH 4.0 and 2.0, which can be attributed to change in polarity upon complexation due to H-bonding of tetrazole moiety with peripheral hydroxyl groups of β-CD.[20,21] Absorption spectra obtained for LMT at different pH values in the presence of β-CD (i.e. 5 mmol L^{-1}) showed an isosbestic point at 290 nm, indicating that two different species, $HLMT^{+}$-βCD and LMT-βCD, exist at equilibrium (Figure 6). In the absence of β-CD, a less resolved isosbestic point was found at 287 nm, indicating equilibrium between protonated and neutral LMT species at different pH values, in agreement with earlier reported isosbestic point of LMT.[12,14]

Figure 7 shows that fluorescence emission intensity of LMT gradually increases with increasing β-CD concentration (0–7 mmol L^{-1}) in pH 8.0 buffer solutions. The same fluorescence emission enhancement was

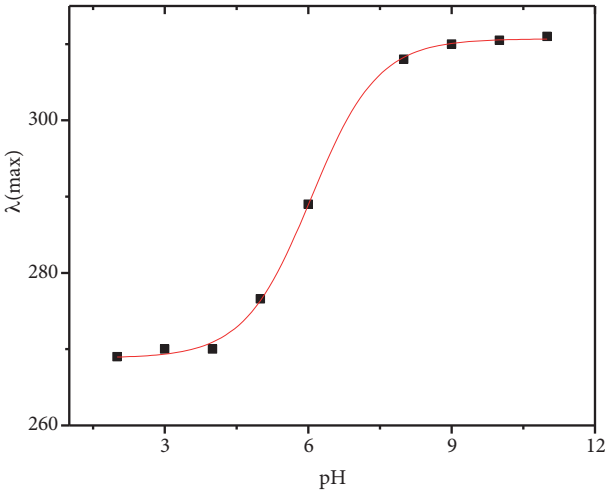

Figure 4. A plot of λ_{max} of absorption spectra of 5.0 $\times$ 10^{-5} mol L^{-1} LMT in 0.10 mol L^{-1} phosphate buffer vs. pH of the buffer solutions.

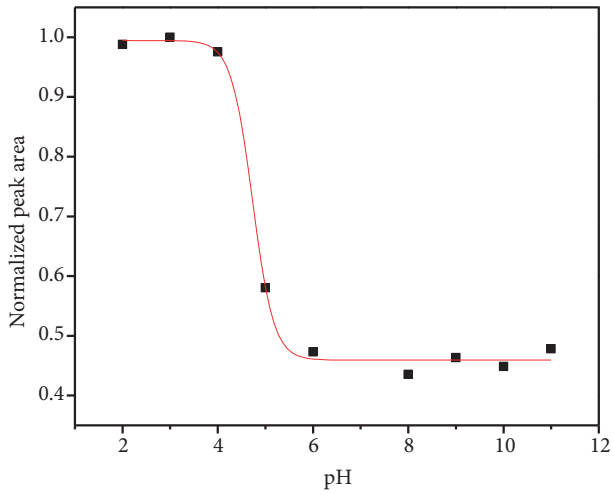

Figure 5. A plot of normalized peak area of fluorescence emission spectra of 5.0 $\times$ 10^{-5} mol L^{-1} LMT in 0.10 mol L^{-1} phosphate buffer vs. pH of the buffer solutions.

obtained for LMT/β-CD complexation in pH 4.0, 5.0, and 6.0 buffer solutions. When LMT is entrapped within the hydrophobic rigid β-CD cavity, its molecular motions are constrained in this more viscous microenvironment, protecting the excited state from nonradiative and quenching processes and enhancing fluorescence emission.[22,23] At pH 2.0, the fluorescence emission spectra show that the band at 502 nm, obtained for protonated LMT, is shifted to 483 nm upon addition of 1 mmol L^{-1} β-CD and then fluorescence emission enhancement gradually increases with increasing concentration of β-CD as shown in Figure 8. This clearly indicates that inclusion of $HLMT^{+}$ within the β-CD cavity prevents the deprotonation process in the excited state.

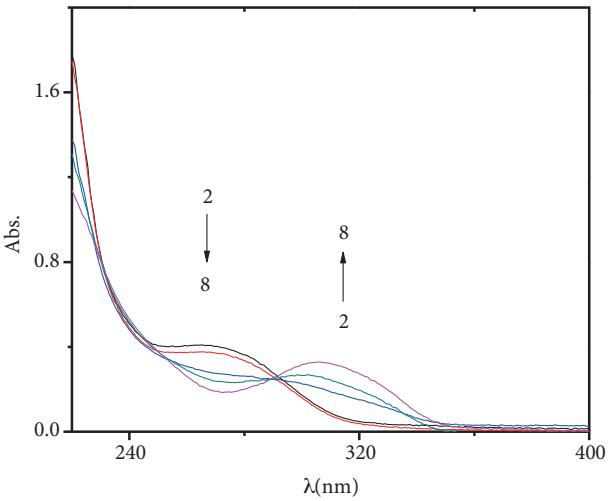

Figure 6. Absorption spectra obtained for LMT in 0.10 mol L^{-1} phosphate buffer at pH 2.0, 4.0, 5.0, 6.0, and 8.0 in the presence of 5 mmol L^{-1} β-CD. An isosbestic point is seen at 290 nm.

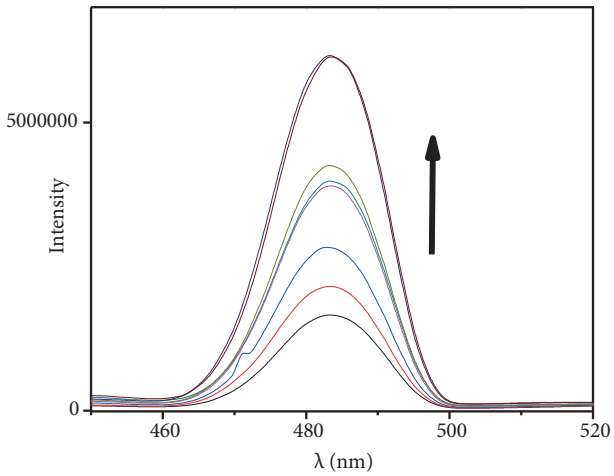

Figure 7. A plot of fluorescence emission spectra of 5.0 $\times$ 10^{-5} mol L^{-1} LMT vs. increasing β-CD concentration (0, 1, 2, 3, 4, 5, 6, and 7 mmol L^{-1}) in 0.10 mol L^{-1} phosphate buffer solutions at pH 8. $\lambda_{excitation}$ = 280 nm.

The ground state acidity constant (pK_a) was determined spectrophotometrically in the presence of β-CD and found to be 5.0, indicating that LMT becomes more acidic in the β-CD cavity, due to H-bonding of the diamino-1,2,4-triazine moiety with β-CD hydroxyl groups. These results clearly indicate that the diamino-1,2,4-triazine moiety is included within the β-CD cavity interacting through H-bonding with the peripheral primary O(6)-H directed at the narrow rim of β-CD, as H-bonding is usually restricted to these easily rotating primary O(6)-H groups,[24] while the 2,3-dichlorophenyl moiety stays at the wide rim of the hydrophobic cavity.

2.3. Evaluation of LMT/β-CD complex formation

The binding constant and the stoichiometry of the LMT/β-CD inclusion complex were obtained from the Benesi–Hildebrand equation using fluorescence emission enhancements of LMT upon increasing β-CD concentration. Benesi–Hildebrand analysis for 1:1 and 1:2 stoichiometries gives Eqs. (1) and (2), respectively.[5,25,26]

$$\frac{1}{I-I_o} = \frac{1}{I'-I_o} + \frac{1}{(I'-I_o)\,K_{11}}\frac{1}{[\beta-CD]} \tag{1}$$

$$\frac{1}{I-I_o} = \frac{1}{I'-I_o} + \frac{1}{(I'-I_o)\,K_{12}}\frac{1}{[\beta-CD]^2}, \tag{2}$$

where K_{11} and K_{12} represent the binding constants of the 1:1 and 1:2 complexes, respectively, where I is the emission intensity of LMT solutions with particular β-CD concentration, I_o is the emission intensity of LMT without β-CD, and I' is the emission intensity at the limit of the highest β-CD concentration.

The Benesi–Hildebrand plots assuming 1:1 association (Figure 9) show good linear regressions at all pH values (Table 1), but those for 1:2 associations are curved. Therefore, these results show that the LMT/β-CD complex has a 1:1 stoichiometry for neutral and protonated LMT (the stoichiometric ratio was also confirmed using Job plots at pH 2.0, 6.0, and 8.0 (Figure 10). As evident from Table 1, protonated and neutral LMT

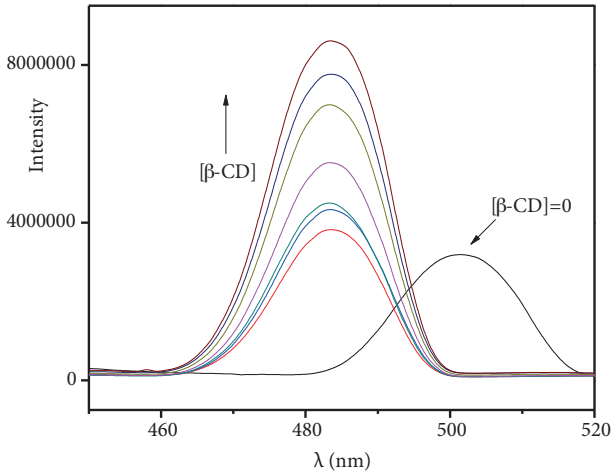

Figure 8. A plot of fluorescence emission spectra of 5.0×10^{-5} mol L^{-1} LMT vs. increasing β-CD concentration (0, 1, 2, 3, 4, 5, 6, and 7 mmol L^{-1}) in 0.10 mol L^{-1} phosphate buffer solutions at pH 2.0. $\lambda_{excitation}$ = 280 nm.

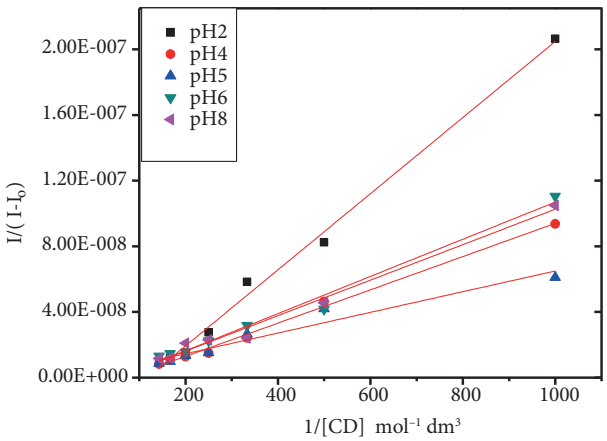

Figure 9. Benesi–Hildebrand plots assuming 1:1 association of LMT/β-CD complexes obtained in 0.10 mol L^{-1} phosphate buffer solutions at different pH values.

forms stable complex with β-CD with complex association constants, K_{11}, ranging from 122 at pH 2.0 to 50.8 at pH 8.0. Table 1 also shows a gradual decrease in complex association constants as pH increases, which indicates that more favorable H-bonding interactions exist between protonated 1,2,4-triazine moiety of $HLMT^+$ and peripheral hydroxyl groups of β-CD.

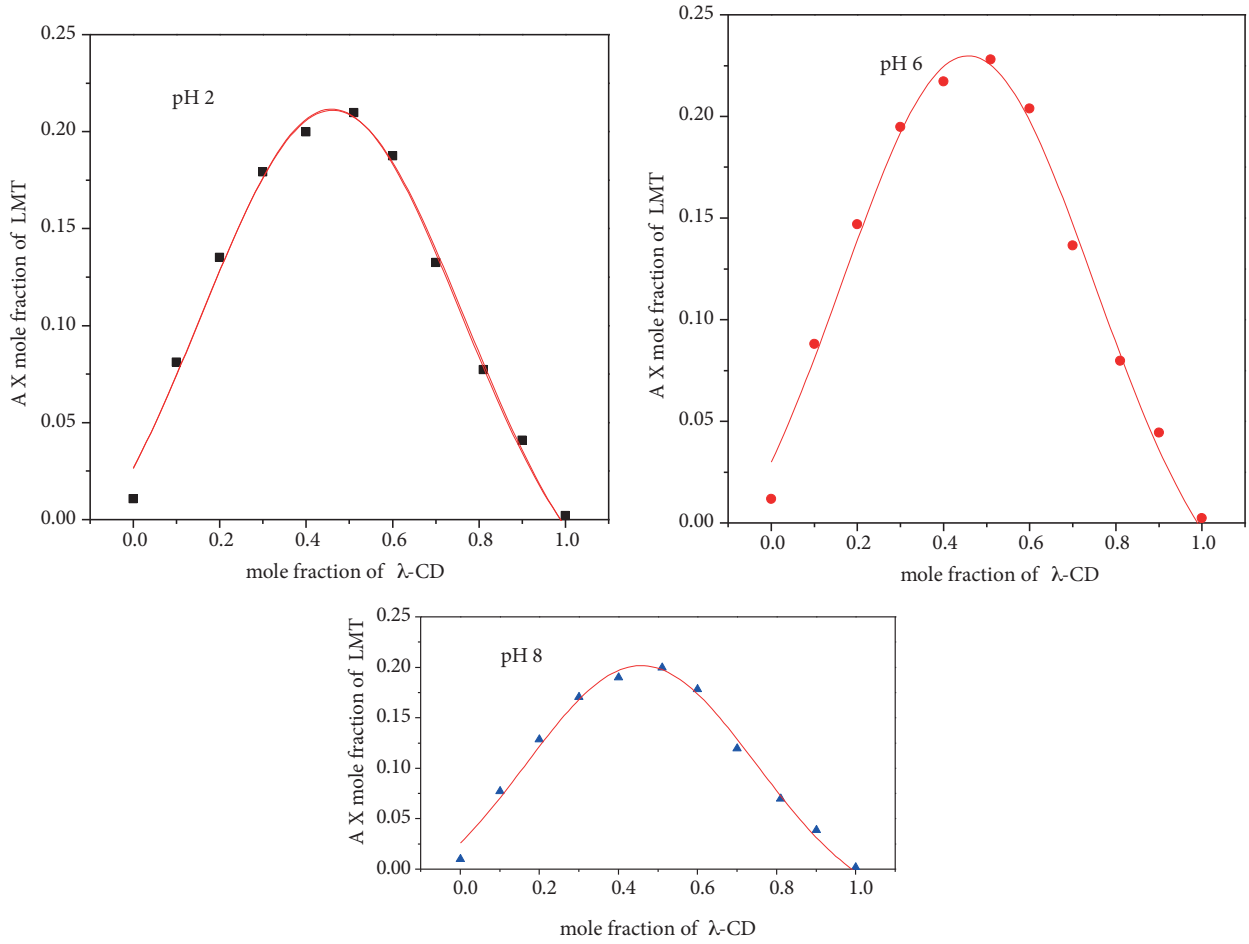

Figure 10. Job plots corresponding to the 1:1 binary combination of LMT/β-CD complexes obtained at different pH values.

Table 1. Association constants, K_{11}, of LMT/β-CD complex, determined by Benesi–Hildebrand analysis, at different pH values at 298.0 ± 0.1 K*.

pH	T/K	K_{11}	R^2
2.0	298.0	122 ± 6	0.980
4.0	298.0	72.3 ± 8	0.994
5.0	298.0	31.2 ± 4	0.939
6.0	298.0	55.6 ± 8	0.936
8.0	298.0	50.8 ± 2	0.984

*±Uncertainties were estimated from regression analysis for a 95% confidence level.

2.4. Evaluation of thermodynamic results

The thermodynamic parameters (ΔH°, ΔS°, and ΔG°) for the formation of LMT/β-CD inclusion complex were determined using the Benesi–Hildebrand K_{11} values of β-CD with protonated and neutral LMT determined at three different temperatures at pH 2.0 and pH 8.0. Gibbs and van't Hoff equations were used to estimate these thermodynamic parameters according to Eqs. (3) and (4), using association constants in the dimensionless mole fraction units, K_{11}^x.[27]

$$\Delta G^\circ = \Delta H^\circ - T\,\Delta S^\circ \tag{3}$$

$$\ln K_{11}^x = -\frac{\Delta H^\circ}{RT} + \frac{\Delta S^\circ}{R} \tag{4}$$

The linear plots of $\ln K_{11}^x$ versus $1/T$ (correlation coefficient = 0.979 at pH 2.0 and 0.999 at pH 8.0) were used to give ($\Delta H^\circ = -R\times$ slope) and ($\Delta S^\circ = R\times$ intercept), while ΔG° was obtained at each temperature using ($\Delta G^\circ = -RT \ln K_{11}^x$). These thermodynamic parameters are listed in Table 2. By careful inspection of the thermodynamic data in Table 2, it is clear that K_{11} values decreased with the rise in temperature at pH 2.0 and pH 8.0, which indicated that the complexation process between β-CD and LMT or HLMT$^+$ was favorable at lower temperature. The results also suggest that complex formation at pH 2.0 and pH 8.0 ($\Delta G^\circ = -21.9$ kJ mol^{-1} for HLMT$^+$/β-CD and –19.7 kJ mol^{-1} for LMT/β-CD) is largely driven by enthalpy ($\Delta H^\circ = -23.1$ kJ mol^{-1} for HLMT$^+$/β-CD and –24.1 kJ mol^{-1} for LMT/β-CD), which is attributed to van der Waals interactions, H-bonding between the guest and host, or due to release of water molecules from the cavity of β-CD on complexation. Table 2 also shows that complex formation of LMT with β-CD at pH 2.0 and 8.0 has negative entropy change ($\Delta S^\circ = -14.9$ J mol^{-1} K^{-1} for HLMT$^+$/β-CD and –4.5 J mol^{-1} K^{-1} for LMT/β-CD), which can be attributed to the limit of the β-CD cavity to the translational and rotational degrees of freedom of the guest molecule.[21,22,27] Our thermodynamic results are in good agreement with the theoretically calculated thermodynamic parameters of LMT/β-CD gas-phase complexation obtained by Seridi and Boufelfel.[28]

Table 2. The association constants of LMT/β-CD complex (K_{11}) and thermodynamic parameters for the binding of LMT to β-CD at pH 2.0 and pH 8.0*.

pH	T(K)	K_{11}	βG (kJ mol^{-1})	βH (kJ mol^{-1})	βS (J mol^{-1} K^{-1})
2.0	298.0	122 ± 6	–21.9 ± 0.1	–23.1 ± 0.4	–4.5 ± 1.5
	303.0	98.2 ± 3	–21.7 ± 0.1		
	313.0	77.1 ± 6	–21.8 ± 0.2		
8.0	298.0	50.8 ± 2	–19.7 ± 0.1	–24.1 ± 0.1	–14.9 ± 0.7
	303.0	42.7 ± 3	–19.6 ± 0.2		
	310.0	31.8 ± 1	–19.5 ± 0.1		

*±Uncertainties were estimated from regression analysis for a 95% confidence level.

2.5. Molecular modeling

Calculations by the MM+ force field showed that LMT/β-CD complex formation is energetically favorable when inclusion takes place from either the 2,3-dichlorophenyl moiety ($E_{binding}$ = –20.65 kcal mol^{-1}) or diamino-1,2,4-triazine moiety ($E_{binding}$ = –21.71 kcal mol^{-1}). Inspection of the binding energies shows that a slightly more favorable lower energy complex geometry is attained when the diamino-1,2,4-triazine moiety is deeply

included within the β-CD cavity, where it makes favorable H-bonding interactions with the primary O(6)-H groups, in accordance with our spectrofluorimetric results (Figure 11). The more favorable inclusion of diamino-1,2,4-triazine moiety of LMT within the β-CD cavity was also reported elsewhere.[28]

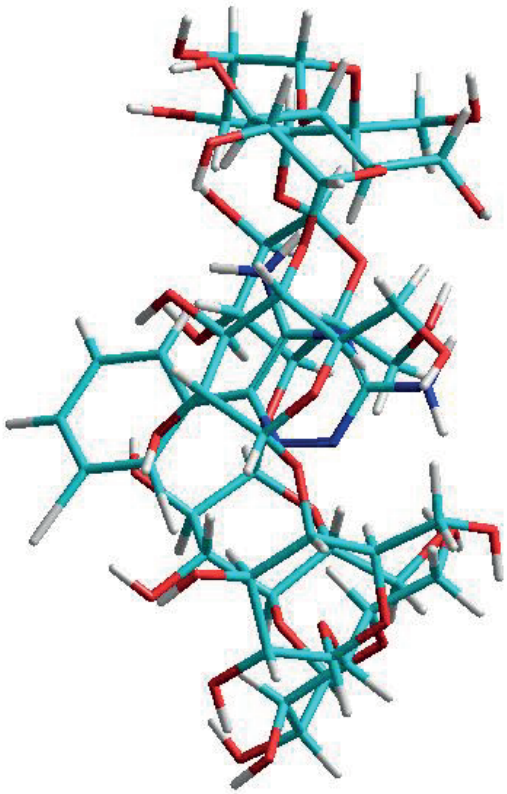

Figure 11. The 1:1 LMT/β-CD minimized complex geometry obtained for the inclusion of diamino-1,2,4-triazine moiety within the β-CD cavity.

3. Conclusions

According to our study, pH value and β-CD have dramatic effects on the spectral properties of LMT. Neutral LMT was found to have a maximum UV-absorption band at 308 nm that is shifted to 268 nm upon protonation at pH 2.0. The fluorescence emission spectra of LMT showed a band at 483 nm at all pH values and a second band at 502 nm at pH 2.0 due to deprotonation of the singlet excited state. The pK_a^* of LMT was found more acidic than pK_a due to intramolecular proton transfer in the excited state. Absorption spectra obtained for LMT at different pH values in the presence of β-CD showed an isosbestic point at 290 nm, while fluorescence emission spectra obtained at different pH values showed intensity enhancement with increasing β-CD concentrations. Benesi–Hildebrand analysis showed that LMT forms 1:1 complex geometries with β-CD in acidic and basic aqueous solutions, while thermodynamic data showed that complex formation of LMT or HLMT$^+$ with β-CD is more favorable at low temperatures and largely driven by enthalpy. Moreover, spectrofluorimetric results and molecular mechanical calculations indicated that LMT is preferentially included within the β-CD cavity through its diamino-1,2,4-triazine moiety.

4. Experimental

4.1. Materials

Lamotrigine (99.6%) was provided by Pharma International Co. (Jordan) and used as received. β-CD (101.0%) was obtained from Wacker Chemie (Germany) and all other chemicals were Sigma-Aldrich analytical grade reagents. Aqueous solutions were prepared using spectroscopic grade water purchased from Merck. Spectroscopic measurements were made in 0.10 mol L^{-1} phosphate buffer solutions containing a fixed concentration of LMT (5.0×10^{-5} mol L^{-1}) and varying concentrations (0–7 mmol L^{-1}) of β-CD. To guarantee the exclusive presence of neutral or cationic species (pKa 5.5–5.7),[29,30] the pH values of the buffered solutions were adjusted to 2.0, 4.0, 5.0, 6.0, and 8.0, respectively. Solutions were freshly prepared to avoid photodecomposition. Since quenching by oxygen was unimportant, fluorescence emission measurements were made with nondegassed solutions. For fluorescence emission measurements, the absorbance of the sample at the excitation wavelengths was less than 0.1 to minimize inner filter effect and reabsorption phenomena. All the spectroscopic measurements were followed at controlled temperature (within ± 0.1 K).

4.2. Instruments

The UV-Vis absorption spectra were recorded on a Specord, S-600 diode-array spectrophotometer interfaced with an HP computer.

Emission spectra were collected using spectrofluorimeter from Edinburgh Analytical Instruments FL 900 S equipped with time correlated single photon counting on FL-900CD; the excitation was provided by an nF900 nanosecond flash lamp filled with H_2, at 0.4 bars and operating at 40 kHz with 6 kV applied across a 1-mm electrode gap.

All pH measurements were made using pH meter benchtop model PL 500, with a stated accuracy of ± 0.01.

4.3. Molecular modeling

Molecular mechanical calculations were performed in a vacuum with HyperChem software (Release 8.0 HyperChem for Windows, Hypercube, Inc. USA) employing an MM+ force field. Energy minimization was performed using the Polak–Ribiere conjugate gradient algorithm with convergence criteria of 0.01 kcal.$mol^{-1}\cdot$Å. The molecular geometry of β-CD was obtained using X-ray diffraction data,[31,32] while LMT structure was built up from standard bond lengths and bond angles, and the resulting structures were then minimized with the MM+ force field. LMT was pushed through the β-CD cavity from the 2,3-dichlorophenyl moiety and the diamino-1,2,4-triazine moiety as starting geometries and the energies of the complex optimal geometries, complex, were calculated and compared with the energy for the separated LMT/βCD pair (Eβ-CD + ELMT) to yield the binding energy, Ebinding, according to Eq. (1).[33]

$$\text{Ebinding} = \text{Ecomplex} - (\text{E}\beta\text{-CD} + \text{ELMT}). \quad (1)$$

Acknowledgments

The authors gratefully acknowledge the financial support extended by the Deanship of Scientific Research at Al Hussein Bin Talal University and would like to thank the University of Al al Bayte for providing the facilities to conduct this work. The authors also thank Pharma International Co., Jordan, for providing the lamotrigine sample as a gift.

References

1. Tekin, S.; Aykut Bingol, C.; Tanridag, T.; Aktan, S. *J. Neural Transm.* **1998**, *105*, 295-303.
2. Nicol Ferrier, I. *British Medical Bulletin* **2001**, *57*, 179-192.
3. Tjia-Leong, E.; Leong, K.; Marson, A. G. *Cochrane Database Syst. Rev.* **2010**, *12*, CD007783.
4. Brewster, M. E.; Loftsson, T. *Adv. Drug. Deliv. Rev.* **2007**. *59*, 645-666.
5. Kim, Y. H.; Cho, D. W.; Song, N. W.; Kim, D.; Yoon, M. *J. Photochem. Photobiol. A, Chem.* **1997**, *106*, 161-167.
6. Muthu Vijayan Enoch, I. V.; Swaminathan, M. *J. Fluoresc.* **2004**, *14*, 751-756.
7. Stalin, T.; Rajendiran, N. *Spectrochim. Acta Part A* **2005**, *61*, 3087-3096.
8. Cox, G. S.; Turro, N. J.; Yang, N. C; Chen, M.J. *J. Am. Chem. Soc.* **1984**, *106*, 422-424.
9. Velasco, J.; Carmona, C.; Munoz, M. A.; Guardado, P.; Balon, M. *J. Incl. Phenom. Macrocycl. Chem.* **1999**, *35*, 637-648.
10. Jahagirdar, K. H.; Bhise, K. S. *Int. J. Pharm. Chem. Sci.* **2014**, *3*, 757-765.
11. Parmar, K. R.; Patel, K. A.; Shah, S. R.; Sheth, N. R. *J. Incl. Phenom. Macrocycl. Chem.* **2009**, *65*, 263-268.
12. Young, R. B.; Chefetz, B.; Liu, A.; Desyaterikd, Y.; Borch, T. *Environ. Sci. Processes Impacts* **2014**, *16*, 848-857.
13. El-Enany, N. M.; El-Sherbiny, D. T.; Abdelal, A. A.; Belal, F. F. *J. Fluoresc.* **2010**, *20*, 463-472.
14. Bilski, P. J.; Wolak, M. A.; Zhang, V.; Moore, D. E.; Chignell, C. F. *Photochem. Photobiol.* **2009**, *85*: 1327-1335.
15. Tajima, S.; Shiobara, S.; Shizuka, H.; Tobita, S. *Phys. Chem. Chem. Phys.* **2002**, *4*, 3376-3382.
16. Takahashi, K. *J. Chem. Soc.; Chem. Commun.* **1991**, 929-930.
17. Gutman, M.; Nachliel, E. *Biochim. Biophys. Acta* **1995**, *1231*, 123-138.
18. Pappayee, N.; Mishra, A. K. *Indian J. Chem.* **2000**, *39A*, 964-973.
19. Wang, Y. H.; Wan, P. *Photochem. Photobiol. Sci.* **2011**, *10*, 1934-1944.
20. García-Padial, M.; Martínez-Ohárriz, M. C.; Isasi, J. R.; Vélaz, I.; Zornoza, A. *J. Incl. Phenom. Macrocycl. Chem.* **2013**, *75*, 241-246.
21. Rajamohan, R.; Nayaki, S. K.; Swaminathan, M. *J. Solution Chem.* **2011**, *40*, 803-817.
22. Vasquez, J. M.; Vu, A.; Schultz, J. S.; Vullev, V. I. *Biotechnol. Prog.* **2009**, *25*, 906-914.
23. Zhang, Q. F.; Jiang, Z. T.; Guo, Y. X.; Li, R. *Spectrochim. Acta, Part A* **2008**, *69*, 65-70.
24. Liu, L.; Guo, Q. X. *J. Incl. Phenom. Macrocycl Chem.* **2002**, *42*, 1-14.
25. Velasco, J.; Guardado, P.; Carmona, C.; Munoz, M. A.; Balon, M. *J. Chem. Soc.; Faraday Trans.* **1998**, *94*, 1469-1476.
26. Benesi, H. A.; Hildebrand, J. H. *J. Am. Chem. Soc.* **1949**, *71*, 2703-2707.
27. Al Omari, M. M.; Daraghmeh, D. H.; El-Barghouthi, M. I.; Zughul, M. B.; Chowdhry, B. Z.; Leharne, S. A.; Badwan, A. A. *J. Pharm. Biomed. Anal.* **2009**, *50*: 449-458.
28. Seridi, L.; Boufelfel, A. *J. Mol. Liq.* **2011**, *158*, 151-158.
29. Rahman, Z.; Zidan, A. S.; Samy, R.; Sayeed, V. A.; Khan, M. A. *AAPS Pharm. Sci. Tech.* **2012**, *13*, 793-801.
30. Chadha, R.; Saini, A.; Arora, P.; Jain, D. S.; Dasgupta, A.; Row, T. N. G. *Cryst. Eng. Comm.* **2011**, *13*, 6271-6284.
31. Saenger, W.; Jacob, J.; Gessler, K.; Steiner, T.; Hoffman, D.; Sanbe, H.; Koizumi, K.; Smith, S. M.; Takaha, T. *Chem. Rev.* **1998**, *98*, 1787-1802.
32. Harata, K. *Bull. Chem. Soc. Jpn.* **1987**, *60*, 2763-2767.
33. Madrid, J. M.; Mendicuti, F.; Mattice, W. L. *J. Phys. Chem. B* **1998**, *102*, 2037-2044.